A&A 445, 1165–1168 (2006)
DOI: 10.1051/0004-6361:20054152

Astronomy & Astrophysics

The FERRUM project: improved experimental oscillator strengths in Cr II*

H. Nilsson[1], G. Ljung[1], H. Lundberg[2], and K. E. Nielsen[3,4]

[1] Atomic Astrophysics, Lund Observatory, Lund University, Box 43, 221 00 Lund, Sweden
[2] Atomic Physics, Department of Physics, Lund Institute of Technology, Box 118, 221 00 Lund, Sweden
[3] Catholic University of America, Washington, DC 20064, USA
[4] Exploration of the Universe Division, Code 667, Goddard Space Flight Center, Greenbelt, MD 20771, USA

Received 5 September 2005 / Accepted 14 September 2005

ABSTRACT

We report absolute oscillator strengths for 119 Cr II transitions in the wavelength region 2050−4850 Å. The transition probabilities have been derived by combining radiative lifetimes, measured with time-resolved laser induced fluorescence, and branching fractions from intensity calibrated Fouirer transform spectrometer data. New radiative lifetimes for the $3d^4(^5D)4p\ ^4F$, ^4D and ^6P terms are reported, adding up to a total of 25 energy levels with measured lifetimes used to derive this improved set of atomic data.

Key words. atomic data – line: identification

1. Introduction

A spectroscopic analysis of an astronomical object is highly dependent on accurate atomic data, such as wavelengths, oscillator strengths and broadening parameters. Lines of the iron-group elements are usually very strong in stellar and nebular spectra, and for objects with enhanced metallicities compared to the solar values they dominate parts of the observed spectrum. Cr II is shown to be very strong in spectra of Chemically Peculiar stars and shows for a few stars, such as 17 Com, an abundance enhancement of several orders of magnitude (Rice & Wehlau 1994). For those objects it is important to have a good understanding of the Cr II spectrum to get accurate results from the stellar analysis. In objects with an effective temperatures in the range 5000 to 10 000 K chromium is predominantly singly ionized.

An investigation of the chemical composition of an astronomical object is dependent on the population distrubition within the atoms energy level systems and the transition probabilities of the studied spectral lines. To understand how the energy levels are populated knowledge of the local excitation conditions is needed. For well behaving stars most lines can be assumed to be formed in the interior of the photosphere under local thermodynamic equlibrium, i.e. the population obeys the Boltzmann and Saha distribution laws. With a known level population the reliability of the abundance analysis will be solely dependent on the accuracy of the atomic data. For more complex stellar atmospheres with inhomogenous abundance patterns, it is possible to probe the atmospheric conditions at different depths by using a large set of lines from different parts of the energy level system.

The purpose of this paper is to provide a complete set of wavelengths and oscillator strengths from the 25 lowest odd energy levels. We present oscillator strengths for 119 lines derived from line intensity ratios from Fourier transform (FT) spectra combined with lifetimes from time-resolved laser-induced fluorescence (LIF) measurements. Using the same technique previous experimental determinations of lifetimes for Cr II levels have been made by e.g. Schade et al. (1990), Pinnington et al. (1993) and Bergeson & Lawler (1993), whereas Engman et al. (1975) and Pinnington et al. (1973) used the beam-foil technique. Earlier experimentally determined transition probabilities in Cr II have been; Bergeson & Lawler (1993) combining branching fractions (BFs) and measured lifetimes; Spreger et al. (1994) using branching ratios combined with arc-emission intensities; Gonzalez et al. (1994) using a laser produced plasma to determine emission-line intensities; Musielok & Wujec (1979), Wujec & Weniger (1981) and Goly & Weniger (1980) using arc emission.

We present an improved, more complete set of data including new lifetimes for seven energy levels and accurately measured BFs for 119 Cr II transitions. For energy levels with no new lifetime measurements, data from Bergeson & Lawler (1993) and Schade et al. (1990) have been incorporated into the analysis.

* Tables 1–3 are only available in electronic form at
http://www.edpsciences.org

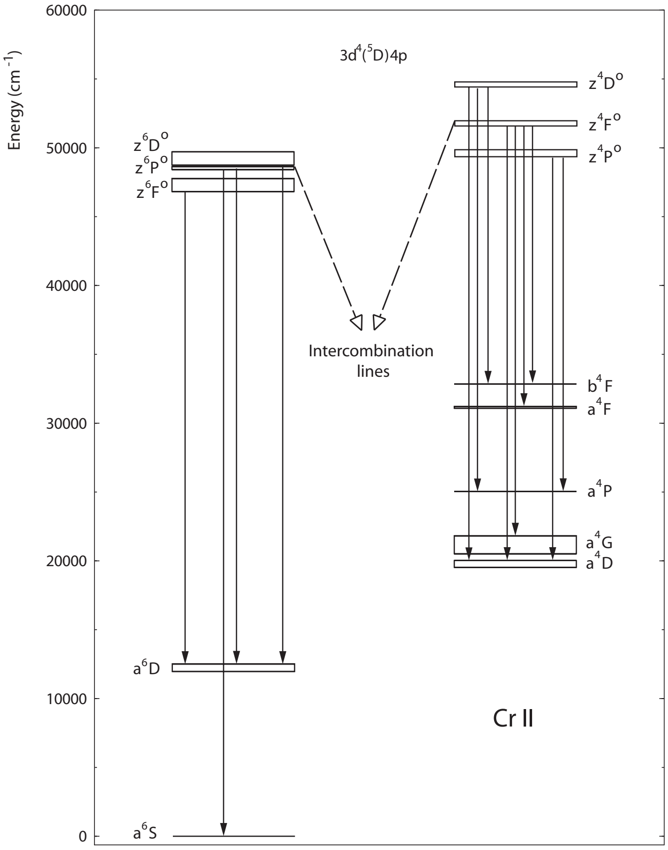

Fig. 1. A partial level diagram of Cr II showing the levels investigated in this work. Left hand side shows the sextet levels and right hand the quartets. Since the LS-coupling in Cr II is not pure, intercombination lines are seen between the quartet and sextet systems.

2. The Cr II spectrum

Singly ionized chromium has five valence electrons outside an argon core. As in the other iron-group elements the lowest even levels belong to the configuration complex $(3d + 4s)^5$. All upper levels included in this analysis belong to $3d^4(^5D)4p$ with the same parent term ^{5}D, giving a total of 25 odd levels in an energy range between 47 000 and 55 000 cm^{-1}. Those levels are, as presented in Fig. 1, grouped in six terms; ^{6}F, ^{6}D, ^{6}P, ^{4}F, ^{4}D and ^{4}P, where the sextets can, with permitted LS transitions, combine with the $3d^5\ ^6S_{5/2}$ and $3d^4(^5D)4s\ ^6D$ terms at zero and $\sim$12 000 cm^{-1}, respectively. This produces two sets of strong lines; the first to the ground state with transitions at 2000 Å and a second at 2600 Å. The strongest lines within the quartet system fall in the wavelength region 2800 to 3500 Å.

The complex energy level system prevents a good description of the spectrum based on pure LS coupling, which is evident by the presence of intercombination lines in the spectrum. The contribution to the total BF from the intercombination lines is derived to be approximately 20% from the $z^6D^o_{1/2}$, $z^6D^o_{3/2}$ and $z^6D^o_{5/2}$ levels, but small (<1%) from $z^6D^o_{7/2}$ and $z^6D^o_{9/2}$. Strong intercombination lines, contributing as much as 50% to the total BF, are seen from z^4P^o term, indicating level mixing beween z^6D^o and z^4P^o.

3. Oscillator strengths

The oscillator strength, f, is related to the transition probability, A, according to,

$$f = 1.499 \times 10^{-16} \frac{g_i}{g_k} \lambda^2 A_{ik},$$

where g_i and g_k are the statistical weights for the upper and lower level, respectively, λ is the transition wavelength in Å, and A_{ik} is the transition probability from level i to k in s^{-1}. The transition probability is derived from the branching fraction (BF) and the radiative lifetime for the upper level (τ_i) as,

$$A_{ik} = \frac{(BF)_{ik}}{\tau_i}.$$

The uncertainty in the transition probability is dependent on the uncertainty in the intensity and the lifetime measurements. The total relative uncertainty of the transition probability A_{ik} for line is described in Sikström et al. (2002), where the uncertainty in the intensity measurements, calibration, self-absorption, missing lines and connection of measurements in different spectra are discussed. This analysis is based on: BFs measured with FT spectroscopy and lifetime measurements using the LIF technique. The experimental techniques for acquiring the atomic parameters are briefly described in the following sections.

3.1. Branching fractions (BFs)

The BF of an emission line is related to the transition probability or the intensity of the line as,

$$(BF)_{ik} = \frac{A_{ik}}{\sum_j A_{ij}} = \frac{I_{ik}}{\sum_j I_{ij}},$$

where A_{ik} is the transition probability for the line from level i to level k, and I_{ik} is the measured intensity for the line. The sums are over all possible decay channels from the level i. The spectral line intensities were measured in spectra obtained with the Chelsea Instrument FT500 UV FT spectrometer in Lund, using a hollow cathode discharge lamp as light source. A cathode containing chromium was employed using argon as carrier gas. Spectra were recorded at currents ranging from 100 to 600 mA with an argon pressure of 1 torr in the spectral intervals 18 000–36 000 cm^{-1} and 30 000–60 000 cm^{-1}. The intensity measurements were made by fitting a Voigt profile to each spectral line, where the calculated equivalent width of the fitted line was used as an intensity measure.

The measured line intensity is dependent on the instrumental response, which needs to be established to calibrate the recorded spectra. The instrumental response function can be determined by using either individual carrier gas lines or an external continuous light source. In this analysis both these methods have been used to cover the whole observed spectral region. The internal calibration was utilized using accurately measured Ar II branching ratios from Whaling et al. (1993) and Hashiguchi & Hasikuni (1985) in the spectral region between 18 000–25 000 cm^{-1}, while a calibrated continuous deuterium lamp was used to achieve the response function above 25 000 cm^{-1}.

Strong lines to low energy states can be affected by self-absorption, i.e. photons can be re-absorbed in the high-density ion plasma. To investigate if the lines are subject for self-absorption the line intensities were measured under different plasma conditions. Interferograms with currents ranging between 100 and 600 mA (in steps of 100 mA) were recorded with a constant carrier gas pressure in the hollow cathode discharge lamp. The intensity ratios of spectral lines from the same upper level were plotted as a function of the current, where the slope of the graph shows the influence of self-absorption. Only the resonance lines were shown to be affected by self-absorption. To decrease the self-absorption in the resonance lines a small piece of chromium was put inside an iron cathode, thus decreasing the chromium density in the hollow cathode plasma. With this set-up no sign of self-absorption was observed.

The equivalent widths were measured in two different spectral regions, that had to be connected to set the intensity calibration on the same scale. By measuring many lines in the overlapping region (30 000−36 000 cm^{-1}), a normalization factor was calculated based on the intensity ratio for the lines measured in both spectral region.

The BF is dependent of intensity measurements for all lines from the same upper level. If some lines are either too weak to be measured accurately or are transitions outside the recorded spectral interval the total intensity will be underestimated and give a too large BF. The BF residual was calculated using the Cowan code (Cowan 1981). Since the calculated BFs were considered to be in reasonable agreement with the experimental values, the Cowan code was assumed to give a satisfactory estimate of the residual.

3.2. Lifetimes

Radiative lifetimes for ten levels, including three previously measured, have been obtained at Lund Laser Centre using time-resolved LIF. A plasma cone consisting of chromium atoms and ions was created by radiating pulses from Nd:YAG ablation laser onto a rotating chromium target located in a vacuum chamber. To produce the desired pumping wavelengths a Nd:YAG pumped dye-laser was used together with frequency doubling/tripling crystals in combination with a Stoke-shifting H_2 cell. With this setup we could produce laser pulses to excite the ions by a single-step excitation from metastabile even states, to the target levels. The fluorescence from the levels was filtered with a 20 cm monochromator and detected by a photomultiplier tube. The time-resolved signal was averaged over 1024 pulses to increase the signal-to-noise ratio. In order to evaluate the lifetimes the LIF signal was fitted with a convolution of the recorded laser signal and an exponential decay curve. An average of 10−20 recordings were used to derive the lifetime for each level. For a comprehensive discussion of the LIF technique see Li et al. (2000).

4. Results and discussion

We have derived 119 oscillator strengths in Cr II by combining experimental lifetimes and BFs. The $\log gf$ values are compared with previous measurements by Bergeson & Lawler (1993), Gonzalez et al. (1994), Spreger et al. (1994), Musielok & Wujec (1979) and Kurucz (1988). The agreement between our work and Bergeson & Lawler (1993) and Gonzalez et al. (1994) is within the uncertainties as seen in Figs. 2 and 3. One exception is noticed; the transition $a^6D_{5/2} - z^6F^o_{3/2}$ at 2876 Å, where the difference between our value and the value from Gonzalez et al. (1994) is −0.255. The agreement between our work and the results from Spreger et al. (1994) and Musielok & Wujec (1979) is, as presented in Figs. 4 and 5 not as distinct.

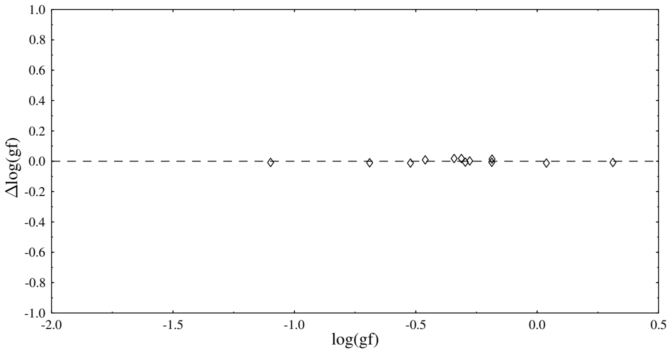

Fig. 2. Comparision between log gf-values from our work and the work of Bergeson & Lawler (1993). $\Delta\log(gf) = \log(gf)_{\rm This\,Work} - \log(gf)_{\rm Bergeson}$ is plotted as a function of line strength.

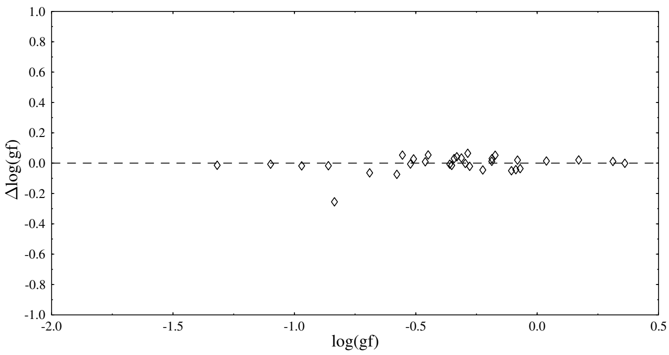

Fig. 3. Comparision between log gf-values from our work and the work of Gonzalez et al. (1994). $\Delta\log(gf) = \log(gf)_{\rm This\,Work} - \log(gf)_{\rm Gonzales}$ is plotted as a function of line strength.

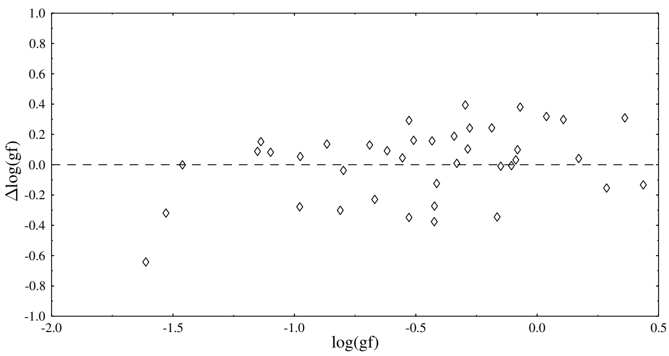

Fig. 4. Comparison between log(gf) values from our work and the work of Spreger et al. (1994). $\Delta\log(gf) = \log(gf)_{\rm This\,Work} - \log(gf)_{\rm Spreger}$ is plotted as a function of line strength.

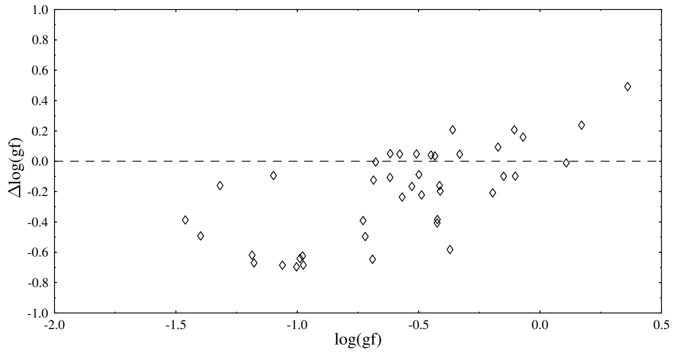

Fig. 5. Comparision between log gf-values from our work and the work of Musielok & Wujec (1979). $\Delta\log(gf) = \log(gf)_{\text{This Work}} - \log(gf)_{\text{Musielok}}$ is plotted as a function of line strength.

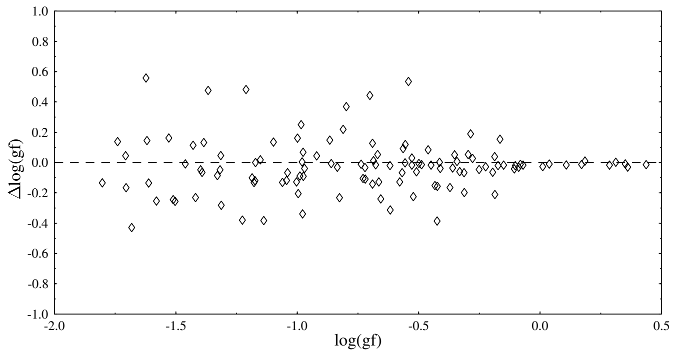

Fig. 6. Comparision between log gf-values from our work and Kurucz (1988). $\Delta\log(gf) = \log(gf)_{\text{This Work}} - \log(gf)_{\text{Kurucz}}$ is plotted as a function of line strength.

Information about the energy levels, observed transitions, measured BFs and calculated uncertainties are presented in Table 1. The levels investigated in this work, the wavelength of the observed fluorescence, the conversion scheme for the excitation laser and the measured radiative lifetimes determined are given in Table 2. Table 3 is a finding list where our results are sorted by air wavelength and compared to previous results.

One case of wavelength coincidence of lines from different energy level combinations is observed. The transitions $a^6\mathrm{D}_{7/2} - z^6\mathrm{D}^{\mathrm{o}}_{7/2}$ and $a^6\mathrm{D}_{9/2} - z^6\mathrm{D}^{\mathrm{o}}_{9/2}$ differ by 0.03 cm^{-1} only, and cannot be resolved in our spectra. Theoretical branching fractions are used to derive oscillator strengths for those lines. The uncertainties of the blended lines are not given in Table 1. However, to estimate the uncertainties of the other lines in the same group the blended lines were included as residuals with an uncertainty of 50%. This is reflected by the large uncertainty of the other lines, spanning between 23 and 42%. The BFs and intensities of the unblended lines in the two groups were used to calculate the intencity of the blended lines and compared with the experimental feature in the spectra. This comparison agreed with in less then 10%, which imply that the uncertaities are overestimated.

The wavelengths reported in Tables 1–3 are Ritz wavelengths derived from energy levels from S. Johansson (unpublished), and available in the NIST compilation of the iron group elements (Sugar & Corliss 1985).

Acknowledgements. We greatfully acknowledge Professor S. Johansson for his support and for reading the manuscript and Professor U. Litzén for enlighting discussions.

References

Bergeson, S. D., & Lawler, J. E. 1993, ApJ, 408, 382
Cowan, R. D. 1981, The Theory of Atomic Structure and Spectra (Berkley, CA: University of California)
Engman, B., Gaupp, A., Curtis, L. J., & Martinson, I. 1975, Phys. Scr, 12, 220
Goly, A., & Weniger, S. 1980, J. Quant. Spec. Radiat. Transf., 24, 335
Gonzalez, A. M., Ortiz, M., & Campos, J. 1994, Can. J. Phys., 72, 57
Hashiguchi, S., & Hasikuni, M. 1985, JPSJ, 54, 1290
Kurucz, R. L. 1988, in Trans. IAU, XXB, ed. McNally (Kluwer: Dordrecht), 168
Li, Z. S., Lundberg, H., Wahlgren, G. M., & Sikström, C. M. 2000, Phys. Rev. A, 62, 032505
Musielok, J., & Wujec, T. 1979, A&AS, 38, 119
Pinnington, E. H., Ji, Q., Gou, B., et al. 1993, Can. J. Phys., 71, 470
Pinnington, E. H., Lutz, H. O., & Carriaveao, G. W. 1973, Nucl. Instrum. Methods, 110, 55
Rice, J. B., & Wehlau, W. H. 1994, A&A, 291, 825
Schade, W., Mundt, B., & Helbig, V. 1990, Phys. Rev. A, 42, 1454
Sikström, C. M., Nilsson, H., Litzén, U., Blom, A., & Lundberg, H. 2002, J. Quant. Spec. Radiat. Transf., 74, 355
Spreger, R., Schelm, B., Kock, M., Neger, T., & Ulbel, M. 1994, J. Quant. Spec. Radiat. Transf., 51, 779
Sugar, J., & Corliss, C. 1985, J. Phys. Chem. Ref. Data, 14, Suppl. 2
Whaling, W., Carle, M. T., & Pitt, M. L. 1993, J. Quant. Spec. Radiat. Transf., 50, 7
Wujec, T., & Weniger, S. 1981, J. Quant. Spec. Radiat. Transf., 25, 167

Online Material

Table 1. Cr II BFs and *A*-values. Transitions sorted by upper level.

Upper level	Lower level	σ (cm^{-1})	λ_{air} (Å)	BF Theory[b]	BF Exp.	A^a (10^7 s^{-1})	Unc. (%)
$4p(^5D)\ ^6F_{1/2}$	$4s(^5D)\ ^6D_{1/2}$	34 861.58	2867.645	0.78	0.76	17.70	3
	$4s(^5D)\ ^6D_{3/2}$	34 790.81	2873.479	0.22	0.24	5.57	6
	Residual				0.00		
$4p(^5D)\ ^6F_{3/2}$	$4s(^5D)\ ^6D_{1/2}$	34 943.36	2860.934	0.31	0.30	7.24	5
	$4s(^5D)\ ^6D_{3/2}$	34 872.59	2866.740	0.57	0.57	13.60	3
	$4s(^5D)\ ^6D_{5/2}$	34 757.35	2876.245	0.12	0.12	2.95	5
	Residual				0.01		
$4p(^5D)\ ^6F_{5/2}$	$4s(^5D)\ ^6D_{3/2}$	35 007.77	2855.670	0.47	0.47	11.30	4
	$4s(^5D)\ ^6D_{5/2}$	34 892.53	2865.102	0.47	0.46	11.10	4
	$4s(^5D)\ ^6D_{7/2}$	34 736.49	2877.973	0.06	0.06	1.44	6
	Residual				0.01		
$4p(^5D)\ ^6F_{7/2}$	$4s(^5D)\ ^6D_{5/2}$	35 079.42	2849.837	0.63	0.62	15.20	3
	$4s(^5D)\ ^6D_{7/2}$	34 923.38	2862.571	0.35	0.36	8.66	5
	$4s(^5D)\ ^6D_{9/2}$	34 730.80	2878.444	0.02	0.02	0.48	8
	Residual				0.00		
$4p(^5D)\ ^6F_{9/2}$	$4s(^5D)\ ^6D_{7/2}$	35 160.69	2843.249	0.81	0.80	18.90	3
	$4s(^5D)\ ^6D_{9/2}$	34 968.11	2858.909	0.19	0.20	4.87	6
	Residual				0.00		
$4p(^5D)\ ^6F_{11/2}$	$4s(^5D)\ ^6D_{9/2}$	35 255.18	2835.629	1.00	1.00	25.00	3
	Residual				0.00		
$4p(^5D)\ ^6D_{1/2}$	$4s(^5D)\ ^6D_{1/2}$	37 530.96	2663.675	0.20	0.18	4.29	8
	$4s(^5D)\ ^6D_{3/2}$	37 460.19	2668.707	0.67	0.62	14.50	8
	$4s(^5D)\ ^4D_{1/2}$	29 964.52	3336.321	0.06	0.09	2.02	14
	$4s(^5D)\ ^4D_{3/2}$	29 861.60	3347.820	0.06	0.09	2.10	14
	Residual				0.02		
$4p(^5D)\ ^6D_{3/2}$	$4s(^5D)\ ^6D_{1/2}$	37 602.79	2658.586	0.33	0.26	6.24	8
	$4s(^5D)\ ^6D_{3/2}$	37 532.02	2663.599	0.01	0.02	0.56	9
	$4s(^5D)\ ^6D_{5/2}$	37 416.78	2671.803	0.51	0.46	10.90	7
	$4s(^5D)\ ^4D_{1/2}$	30 036.35	3328.342	0.01	0.01	0.30	22
	$4s(^5D)\ ^4D_{3/2}$	29 933.43	3339.786	0.04	0.07	1.58	13
	$4s(^5D)\ ^4D_{5/2}$	29 766.72	3358.491	0.09	0.13	3.17	13
	$4s(^5D)\ ^4P_{1/2}$	27 740.76	3603.776	0.01	0.03	0.79	14
	Residual				0.02		
$4p(^5D)\ ^6D_{5/2}$	$4s(^5D)\ ^6D_{3/2}$	37 319.22	2678.789	0.31	0.36	8.02	7
	$4s(^5D)\ ^6D_{5/2}$	37 203.98	2687.087	0.12	0.19	4.29	7
	$4s(^5D)\ ^6D_{7/2}$	37 047.94	2698.405	0.35	0.20	4.39	8
	$4s(^5D)\ ^4D_{5/2}$	29 553.92	3382.675	0.03	0.05	1.02	9
	$4s(^5D)\ ^4D_{7/2}$	29 327.79	3408.757	0.15	0.16	3.61	9
	$3d^5\ ^4P_{5/2}$	27 529.28	3631.461	0.02	0.02	0.50	10
	$3d^5\ ^4P_{3/2}$	27 527.69	3631.671	0.01	0.01	0.18	16
	Residual				0.01		

Table 1. continued.

Upper level	Lower level	σ (cm^{-1})	λ_{air} (Å)	BF Theory[b]	BF Exp.	A^a ($10^7\ s^{-1}$)	Unc. (%)
$4p(^5D)\ ^6D_{7/2}$	$4s(^5D)\ ^6D_{5/2}$	37 497.95	2666.020	0.35	0.35	9.19	23
	$4s(^5D)\ ^6D_{7/2}$	37 341.91	2677.161	0.45	*Bl*[c]	11.90	
	$4s(^5D)\ ^6D_{9/2}$	37 149.33	2691.040	0.20	0.19	5.13	23
	Residual				0.46		
$4p(^5D)\ ^6D_{9/2}$	$4s(^5D)\ ^6D_{7/2}$	37 534.52	2663.422	0.20	0.20	5.28	40
	$4s(^5D)\ ^6D_{9/2}$	37 341.94	2677.159	0.79	*Bl*[c]	20.90	
	$4s(^5D)\ ^4D_{7/2}$	29 814.37	3353.124	0.00	0.01	0.15	42
	Residual				0.79		
$4p(^5D)\ ^6P_{3/2}$	$3d^5\ ^6S_{5/2}$	48 398.95	2065.501	0.39	0.28	11.70	9
	$4s(^5D)\ ^6D_{1/2}$	36 437.14	2743.641	0.16	0.18	7.66	9
	$4s(^5D)\ ^6D_{3/2}$	36 366.37	2748.980	0.25	0.28	11.60	9
	$4s(^5D)\ ^6D_{5/2}$	36 251.13	2757.720	0.19	0.24	9.97	9
	$4s(^5D)\ ^4D_{3/2}$	28 767.78	3475.116	0.00	0.01	0.33	20
	$4s(^5D)\ ^4D_{5/2}$	28 601.07	3495.373	0.00	0.01	0.27	22
	Residual				0.00		
$4p(^5D)\ ^6P_{5/2}$	$3d^5\ ^6S_{5/2}$	48 491.10	2061.575	0.39	0.31	12.80	9
	$4s(^5D)\ ^6D_{3/2}$	36 458.52	2742.032	0.06	0.07	3.02	9
	$4s(^5D)\ ^6D_{5/2}$	36 343.28	2750.727	0.21	0.23	9.56	9
	$4s(^5D)\ ^6D_{7/2}$	36 187.24	2762.589	0.33	0.38	15.90	9
	$4s(^5D)\ ^4D_{7/2}$	28 467.09	3511.824	0.00	0.01	0.31	17
	Residual				0.00		
$4p(^5D)\ ^6P_{7/2}$	$3d^5\ ^6S_{5/2}$	48 632.12	2055.596	0.40	0.31	12.90	9
	$4s(^5D)\ ^6D_{5/2}$	36 484.30	2740.094	0.02	0.02	0.89	12
	$4s(^5D)\ ^6D_{7/2}$	36 328.26	2751.864	0.12	0.13	5.57	9
	$4s(^5D)\ ^6D_{9/2}$	36 135.68	2766.531	0.47	0.54	22.30	9
	Residual				0.00		
$4p(^5D)\ ^4F_{3/2}$	$4s(^5D)\ ^4D_{1/2}$	32 055.90	3118.646	0.57	0.57	13.60	10
	$4s(^5D)\ ^4D_{3/2}$	31 952.98	3128.692	0.21	0.21	5.05	11
	$3d^5\ ^4G_{5/2}$	31 072.09	3217.393	0.18	0.18	4.35	11
	Residual				0.04		
$4p(^5D)\ ^4F_{5/2}$	$4s(^5D)\ ^4D_{3/2}$	32 038.31	3120.359	0.61	0.60	14.60	10
	$4s(^5D)\ ^4D_{5/2}$	31 871.60	3136.681	0.18	0.18	4.36	11
	$3d^5\ ^4G_{7/2}$	31 151.65	3209.176	0.16	0.17	4.19	11
	Residual			1.00	0.05		
$4p(^5D)\ ^4F_{7/2}$	$4s(^5D)\ ^6D_{7/2}$	39 485.02	2531.845	0.00	0.01	0.24	12
	$4s(^5D)\ ^4D_{5/2}$	31 991.00	3124.973	0.69	0.68	16.50	8
	$4s(^5D)\ ^4D_{7/2}$	31 764.87	3147.220	0.10	0.10	2.50	9
	$3d^5\ ^4G_{9/2}$	31 269.55	3197.075	0.16	0.16	3.97	9
	$4s(^3F)\ ^4F_{7/2}$	20 620.30	4848.235	0.01	0.01	0.36	18
	Residual				0.04		

Table 1. continued.

Upper level	Lower level	σ (cm^{-1})	λ_{air} (Å)	BF Theory[b]	BF Exp.	A^a (10^7 s^{-1})	Unc. (%)
$4p(^5D)\ ^4F_{9/2}$	$4s(^5D)\ ^6D_{9/2}$	39 446.26	2534.333	0.01	0.02	0.50	12
	$4s(^5D)\ ^4D_{7/2}$	31 918.69	3132.053	0.78	0.76	18.60	7
	$3d^5\ ^4G_{11/2}$	31 430.60	3180.693	0.17	0.17	4.21	9
	$3d^5\ ^4D_{7/2}$	26 909.00	3715.172	0.00	0.01	0.21	18
	$4s(^3F)\ ^4F_{9/2}$	20 723.35	4824.127	0.01	0.01	0.35	16
	Residual				0.03		
$4p(^5D)\ ^4D_{1/2}$	$4s(^5D)\ ^4D_{1/2}$	34 889.77	2865.328	0.34	0.33	7.73	11
	$4s(^5D)\ ^4D_{3/2}$	34 786.85	2873.806	0.36	0.37	8.50	11
	$3d^5\ ^4D_{1/2}$	29 382.62	3402.396	0.09	0.08	1.88	16
	$3d^5\ ^4D_{3/2}$	29 375.21	3403.254	0.09	0.08	1.93	16
	$3d^5\ ^4F_{3/2}$	21 573.26	4634.070	0.05	0.07	1.63	16
	Residual			1.00	0.07		
$4p(^5D)\ ^4D_{3/2}$	$4s(^5D)\ ^4D_{1/2}$	34 971.27	2858.650	0.16	0.16	3.74	11
	$4s(^5D)\ ^4D_{3/2}$	34 868.35	2867.089	0.28	0.28	6.60	10
	$4s(^5D)\ ^4D_{5/2}$	34 701.64	2880.863	0.26	0.27	6.37	10
	$3d^5\ ^4D_{1/2}$	29 464.12	3392.985	0.05	0.04	0.96	11
	$3d^5\ ^4D_{3/2}$	29 456.71	3393.838	0.07	0.06	1.49	10
	$3d^5\ ^4D_{5/2}$	29 452.76	3394.293	0.07	0.07	1.53	10
	$3d^5\ ^4F_{5/2}$	21 644.57	4618.803	0.04	0.03	0.79	12
	Residual				0.09		
$4p(^5D)\ ^4D_{5/2}$	$4s(^5D)\ ^4D_{3/2}$	34 994.45	2856.757	0.15	0.14	3.28	10
	$4s(^5D)\ ^4D_{5/2}$	34 827.74	2870.432	0.41	0.41	9.55	10
	$4s(^5D)\ ^4D_{7/2}$	34 601.61	2889.192	0.15	0.16	3.70	10
	$3d^5\ ^4P_{5/2}$	32 803.10	3047.606	0.02	0.05	1.24	12
	$3d^5\ ^4P_{3/2}$	32 801.51	3047.754	0.02	0.01	0.32	21
	$3d^5\ ^4D_{7/2}$	29 591.92	3378.331	0.04	0.04	0.85	12
	$3d^5\ ^4D_{3/2}$	29 582.81	3379.371	0.05	0.04	0.97	11
	$3d^5\ ^4D_{5/2}$	29 578.86	3379.822	0.10	0.09	1.99	11
	$3d^5\ ^4F_{7/2}$	21 788.94	4588.199	0.04	0.03	0.79	12
	$3d^5\ ^4F_{5/2}$	21 770.67	4592.049	0.01	0.01	0.20	37
	Residual				0.02		
$4p(^5D)\ ^4D_{7/2}$	$4s(^5D)\ ^4D_{5/2}$	34 986.60	2857.398	0.09	0.09	2.10	11
	$4s(^5D)\ ^4D_{7/2}$	34 760.47	2875.987	0.62	0.66	15.40	10
	$3d^5\ ^4P_{5/2}$	32 961.96	3032.917	0.03	0.02	0.44	20
	$3d^5\ ^4D_{7/2}$	29 750.78	3360.291	0.17	0.14	3.14	12
	$3d^5\ ^4D_{5/2}$	29 737.72	3361.767	0.03	0.03	0.67	13
	$3d^5\ ^4F_{9/2}$	21 930.17	4558.650	0.05	0.04	0.89	12
	Residual				0.02		
$4p(^5D)\ ^4P_{1/2}$	$4s(^5D)\ ^6D_{1/2}$	36 787.55	2717.506	0.06	0.08	1.68	8
	$4s(^5D)\ ^6D_{3/2}$	36 716.78	2722.744	0.19	0.31	6.13	6
	$4s(^5D)\ ^4D_{1/2}$	29 221.11	3421.202	0.34	0.27	5.43	7
	$4s(^5D)\ ^4D_{3/2}$	29 118.19	3433.295	0.33	0.26	5.28	7
	$3d^5\ ^4P_{3/2}$	26 925.25	3712.930	0.06	0.06	1.13	9
	Residual				0.02		

Table 1. continued.

Upper level	Lower level	σ (cm^{-1})	λ_{air} (Å)	BF Theory[b]	BF Exp.	A[a] ($10^7\ s^{-1}$)	Unc. (%)
$4p(^5D)\ ^4P_{3/2}$	$4s(^5D)\ ^6D_{1/2}$	37 044.12	2698.683	0.18	0.29	6.24	6
	$4s(^5D)\ ^6D_{3/2}$	36 973.35	2703.849	0.03	0.04	0.93	7
	$4s(^5D)\ ^6D_{5/2}$	36 858.11	2712.303	0.10	0.17	3.61	6
	$4s(^5D)\ ^4D_{1/2}$	29 477.68	3391.424	0.03	0.03	0.58	11
	$4s(^5D)\ ^4D_{3/2}$	29 374.76	3403.307	0.20	0.15	3.12	7
	$4s(^5D)\ ^4D_{5/2}$	29 208.05	3422.732	0.37	0.25	5.37	6
	$3d^5\ ^4P_{5/2}$	27 183.41	3677.667	0.03	0.02	0.38	11
	$3d^5\ ^4P_{1/2}$	27 182.09	3677.846	0.03	0.02	0.39	11
	$3d^5\ ^4P_{3/2}$	27 181.82	3677.882	0.01	0.01	0.19	19
	Residual				0.02		
$4p(^5D)\ ^4P_{5/2}$	$4s(^5D)\ ^6D_{3/2}$	37 673.75	2653.578	0.20	0.18	3.81	6
	$4s(^5D)\ ^6D_{5/2}$	37 558.51	2661.721	0.12	0.05	1.14	6
	$4s(^5D)\ ^6D_{7/2}$	37 402.47	2672.826	0.08	0.26	5.74	6
	$4s(^5D)\ ^4D_{3/2}$	30 075.16	3324.047	0.01	0.01	0.30	14
	$4s(^5D)\ ^4D_{5/2}$	29 908.45	3342.576	0.10	0.07	1.54	6
	$4s(^5D)\ ^4D_{7/2}$	29 682.32	3368.041	0.40	0.31	6.70	5
	$3d^5\ ^4P_{5/2}$	27 883.81	3585.287	0.05	0.08	1.72	6
	$3d^5\ ^4P_{3/2}$	27 882.22	3585.492	0.02	0.02	0.36	10
	Residual				0.02		

[a] Transition probabilities derived from the experimental BFs and lifetimes presented in Table 2.
[b] Theoretical BFs calculated with the Cowan code (Cowan 1981).
[c] Severly blended line.

Table 2. Measured radiative lifetimes for ten Cr II levels in the $3d^4(^5D)4p$ configuration.

Term	Energy	Observed	Exc. laser	Exp. lifetimes	
		fluorescence	conversion	Our work	Prev. work
	(cm^{-1})	λ_{air} (Å)	scheme[a]	(ns)	(ns)
$^4F_{3/2}$	51 485.15	3118.646	2ω	4.2(4)	
$^4F_{5/2}$	51 669.48	3120.359	2ω	4.1(4)	
$^4F_{7/2}$	51 788.88	3124.973	2ω	4.1(3)	
$^4F_{9/2}$	51 942.70	3132.053	2ω	4.1(3)	
$^4D_{1/2}$	54 418.02	2873.806	$3\omega + S$	4.3(4)	
$^4D_{3/2}$	54 499.52	2867.089	$3\omega + S$	4.3(4)	
$^4D_{5/2}$	54 625.62	2870.432	$3\omega + S$	4.3(4)	
$^4D_{7/2}$	54 784.48	2875.987	$3\omega + S$	4.3(4)	4.20(18)[b]
$^6P_{5/2}$	48 491.10	2762.589	3ω	2.3(2)	2.45(8)[b], 2.5(1)[c], 2.4(2)[d]
$^6P_{7/2}$	48 632.12	2766.531	3ω	2.4(2)	2.4(13)[b], 2.5(1)[c], 2.4(2)[d]

[a] 2ω – frequency doubling, 3ω – frequency tripling, S – Stoke shift.
[b] Pinnington et al. (1993).
[c] Schade et al. (1990).
[d] Bergeson & Lawler (1993).

Table 3. Cr II log gf-values. Lines sorted by wavelength.

λ_{vac} (Å)	σ (cm^{-1})	log gf Our work	Spreger[a]	Bergeson[b]	Gonzalez[c]	Musielok[d]	Kurucz[e]
2056.254	48 632.12	−0.186		−0.20	−0.216		+0.025
2062.234	48 491.10	−0.312		−0.33	−0.346		−0.114
2066.161	48 398.95	−0.522		−0.51	−0.516		−0.297
2532.606	39 485.02	−1.740					−1.878
2535.095	39 446.26	−1.315					−1.361
2654.368	37 673.75	−0.617				−0.667	−0.304
2659.377	37 602.79	−0.578			−0.504	−0.625	−0.450
2662.512	37 558.51	−1.138	−1.29				−0.755
2664.214	37 534.52	−0.251					−0.205
2664.392	37 532.02	−1.623					−2.181
2664.467	37 530.96	−1.040					−0.973
2666.812	37 497.95	−0.106	−0.10		−0.056	−0.313	−0.064
2669.501	37 460.19	−0.509	−0.67		−0.537	−0.557	−0.448
2672.598	37 416.78	−0.331	−0.34		−0.373	−0.377	−0.271
2673.620	37 402.47	−0.433	−0.59			−0.468	−0.281
2677.954	37 341.94	+0.351[f]					+0.360
2677.956	37 341.91	+0.011[f]					+0.038
2679.584	37 319.22	−0.286	−0.39		−0.351		−0.475
2687.884	37 203.98	−0.555	−0.60		−0.608		−0.674
2691.839	37 149.33	−0.352			−0.337		−0.403
2699.205	37 047.94	−0.542					−1.077
2699.484	37 044.12	−0.564					−0.656
2704.651	36 973.35	−1.392					−1.327
2713.107	36 858.11	−0.798	−0.76				−1.167
2718.311	36 787.55	−1.429					−1.543
2723.550	36 716.78	−0.866	−1.002				−1.014
2740.905	36 484.30	−1.098	−1.18	−1.09	−1.091	−1.004	−1.233
2742.843	36 458.52	−0.690	−0.82	−0.68	−0.626		−0.817
2744.453	36 437.14	−0.461		−0.47	−0.470		−0.545
2749.793	36 366.37	−0.278	−0.52	−0.28	−0.257		−0.305
2751.540	36 343.28	−0.187	−0.43	−0.18	−0.199		−0.226
2752.678	36 328.26	−0.296	−0.69	−0.29	−0.294		−0.349
2758.535	36 251.13	−0.342	−0.53	−0.36	−0.372		−0.349
2763.405	36 187.24	+0.038	−0.28	+0.05	+0.024		+0.048
2767.348	36 135.68	+0.312		+0.32	+0.301		+0.310
2836.463	35 255.18	+0.558			+0.562		+0.572
2844.085	35 160.69	+0.361	+0.052		+0.362	−0.131	+0.391
2850.674	35 079.42	+0.171	+0.13		+0.150	−0.067	+0.184
2856.509	35 007.77	−0.081	−0.18		−0.101		−0.069
2857.596	34 994.45	−0.618	−0.71			−0.511	−0.598
2858.237	34 986.60	−0.686				−0.562	−0.698
2859.490	34 971.27	−0.737					−0.726
2859.748	34 968.11	−0.224			−0.179		−0.196
2861.774	34 943.36	−0.449			−0.503	−0.490	−0.432
2863.411	34 923.38	−0.070	−0.45		−0.034	−0.229	−0.053
2865.943	34 892.53	−0.088	−0.12		−0.045		−0.057
2866.170	34 889.77	−0.721					−0.688
2867.582	34 872.59	−0.173			−0.225	−0.266	−0.153
2867.930	34 868.35	−0.488				−0.266	−0.474
2868.487	34 861.58	−0.360			−0.353	−0.567	−0.324
2871.274	34 827.74	−0.150	−0.14			−0.051	−0.133
2874.322	34 790.81	−0.860			−0.843		−0.853
2874.649	34 786.85	−0.677				−0.672	−0.662

Table 3. continued.

λ_{vac}	σ	log gf					
(Å)	(cm^{-1})	Our work	Spreger[a]	Bergeson[b]	Gonzalez[c]	Musielok[d]	Kurucz[e]
2876.831	34 760.47	+0.185					+0.175
2877.089	34 757.35	−0.835			−0.580		−0.804
2878.817	34 736.49	−0.970			−0.952		−0.931
2879.289	34 730.80	−1.318			−1.304	−1.158	−1.270
2881.708	34 701.64	−0.499				−0.411	−0.493
2890.039	34 601.61	−0.556					−0.554
3033.800	32 961.96	−1.313					−1.031
3048.492	32 803.10	−0.984					−1.234
3048.640	32 801.51	−1.580					−1.326
3119.551	32 055.90	−0.102				−0.004	−0.081
3121.263	32 038.31	+0.108	−0.19			+0.119	+0.124
3125.879	31 991.00	+0.286	+0.44				+0.303
3129.599	31 952.98	−0.528	−0.82			−0.362	−0.511
3132.961	31 918.69	+0.437	+0.57				+0.451
3137.590	31 871.60	−0.414	−0.29			−0.254	−0.416
3148.132	31 764.87	−0.528	−0.18				−0.558
3181.613	31 430.60	−0.195				+0.013	−0.131
3197.999	31 269.55	−0.313					−0.246
3210.103	31 151.65	−0.411				−0.214	−0.372
3218.322	31 072.09	−0.568				−0.332	−0.501
3325.003	30 075.16	−1.529	−1.21				−1.691
3329.299	30 036.35	−1.707					−1.752
3337.280	29 964.52	−1.172					−1.172
3340.746	29 933.43	−0.976	−1.03				−1.044
3343.537	29 908.45	−0.811	−0.51				−1.030
3348.782	29 861.60	−1.152	−1.24				−1.170
3354.087	29 814.37	−1.612	−0.97				−1.477
3359.456	29 766.72	−0.669	−0.44				−0.722
3361.256	29 750.78	−0.371				+0.211	−0.206
3362.733	29 737.72	−1.044					−0.926
3369.009	29 682.32	−0.165	+0.18				−0.319
3379.301	29 591.92	−1.061				−0.376	−0.930
3380.341	29 582.81	−1.003				−0.307	−0.875
3380.793	29 578.86	−0.690				−0.044	−0.548
3383.646	29 553.92	−0.978	−0.70			−0.354	−0.639
3392.397	29 477.68	−1.398				−0.906	−1.350
3393.958	29 464.12	−1.178				−0.508	−1.046
3394.812	29 456.71	−0.989				−0.348	−0.900
3395.268	29 452.76	−0.975				−0.291	−0.884
3403.372	29 382.62	−1.186				−0.567	−1.085
3404.231	29 375.21	−1.174					−1.054
3404.283	29 374.76	−0.664					−0.536
3409.735	29 327.79	−0.424	−0.048			−0.017	−0.038
3422.183	29 221.11	−0.720				−0.224	−0.611
3423.714	29 208.05	−0.423	−0.15			−0.039	−0.266
3434.279	29 118.19	−0.729				−0.338	−0.624
3476.111	28 767.78	−1.619					−1.764
3496.373	28 601.07	−1.705					−1.539
3512.828	28 467.09	−1.461	−1.46			−1.074	−1.452
3586.310	27 883.81	−0.701					−1.144
3586.515	27 882.22	−1.385					−1.517
3604.804	27 740.76	−1.211					−1.693
3632.496	27 529.28	−1.226					−0.846

Table 3. continued.

λ_{vac} (Å)	σ (cm^{-1})	log gf Our work	Spreger[a]	Bergeson[b]	Gonzalez[c]	Musielok[d]	Kurucz[e]
3632.706	27 527.69	−1.682					−1.253
3678.714	27 183.41	−1.511					−1.266
3678.893	27 182.09	−1.503					−1.247
3678.930	27 181.82	−1.803					−1.669
3713.986	26 925.25	−1.329					−1.243
3716.229	26 909.00	−1.367					−1.843
4559.928	21 930.17	−0.656					−0.416
4589.484	21 788.94	−0.826					−0.594
4593.336	21 770.67	−1.419					−1.188
4620.096	21 644.57	−0.996					−0.791
4635.368	21 573.26	−0.980					−0.984
4825.475	20 723.35	−0.920					−0.964
4849.590	20 620.30	−0.999					−1.160

[a] Spreger et al. (1994).
[b] Bergeson & Lawler (1993).
[c] Gonzalez et al. (1994).
[d] Musielok & Wujec (1979).
[e] Kurucz (1988).
[f] Blended lines, theoretical BFs used to derive the oscillator strengths.